

Iron(II) Complexes of New Hexadentate 1,1,1-Tris-(iminomethyl)-ethane Podands, and their 7-Methyl-1,3,5-triazaadamantane Rearrangement Products

Sara Diener, Amedeo Santoro, Colin A. Kilner, Jonathan J. Loughrey and Malcolm A. Halcrow*

^aSchool of Chemistry, University of Leeds, Woodhouse Lane, Leeds, UK LS2 9JT.
E-mail: m.a.halcrow@leeds.ac.uk

Electronic Supplementary Information

Figure S1 Views of the asymmetric unit of $[\text{Fe}(\text{IE})][\text{ClO}_4]_2 \cdot 0.7\text{H}_2\text{O}$, showing the ‘A’ and ‘B’ disorder orientations.

Table S1 Selected bond lengths and angles in the crystal structure of $[\text{Fe}(\text{IE})][\text{ClO}_4]_2 \cdot 0.7\text{H}_2\text{O}$

Table S2 Selected bond lengths and angles in the crystal structure of $[\text{Fe}(\text{IF})][\text{BF}_4]_2$.

Table S3 Selected bond lengths and angles in the crystal structure of $[\text{Fe}(\text{IG})][\text{ClO}_4]_2$

Figure S2 View of the dimeric moiety in the crystal structure of $[\text{FeCl}_2(\text{2C})] \cdot n\text{H}_2\text{O}$, showing the complete atom numbering scheme.

Figure S3 Space-filling view of molecule A in $[\text{FeCl}_2(\text{2C})] \cdot n\text{H}_2\text{O}$, showing the steric influence of the ligand methyl substituents on the iron coordination geometry.

Table S4 Selected bond lengths and angles in the crystal structure of $[\text{FeCl}_2(\text{2C})] \cdot n\text{H}_2\text{O}$.

Figure S4 Packing diagram of $[\text{FeCl}_2(\text{2C})] \cdot n\text{H}_2\text{O}$, showing the interdigitation of the dimers through π - π interactions.

Table S5 Metric parameters for the intermolecular π - π interactions in $[\text{FeCl}_2(\text{2C})] \cdot n\text{H}_2\text{O}$

Figure S5 View of the asymmetric unit in the crystal structure of $[\text{2BH}] \text{BF}_4$, showing the hydrogen-bonding interactions in the crystal lattice.

Table S6 Hydrogen bond parameters for the crystal structures in this work.

Figure S6 Energy-minimised molecular model of $[\text{Fe}(\text{2A})_2]^{2+}$, showing the unfavourable steric contacts in the putative molecule.

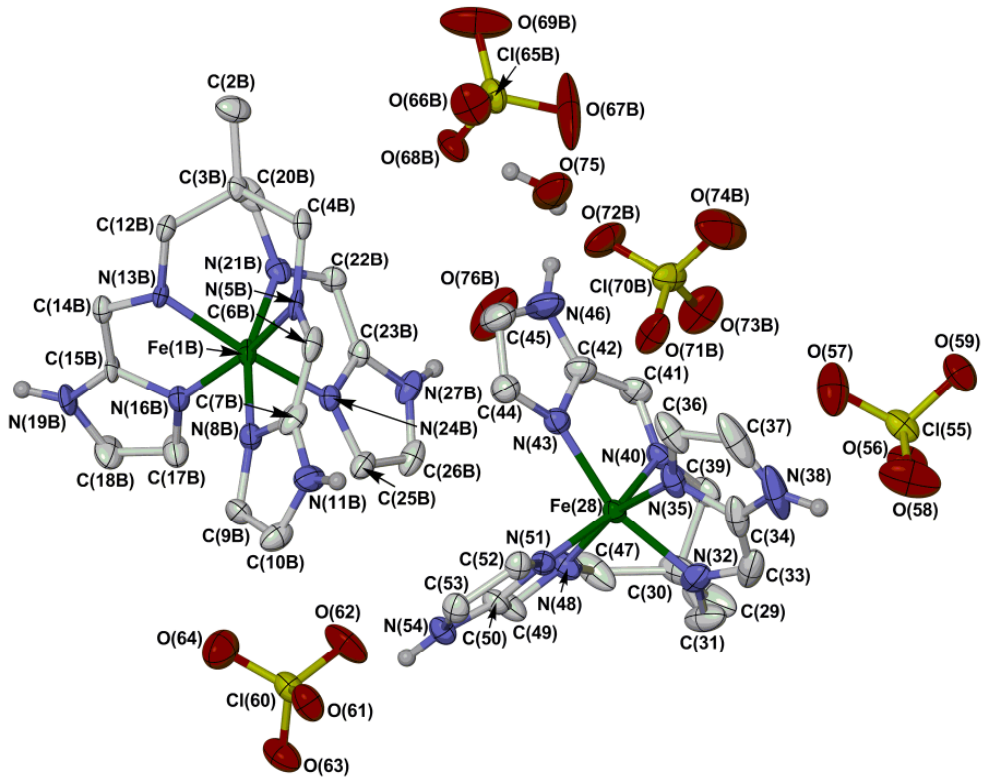
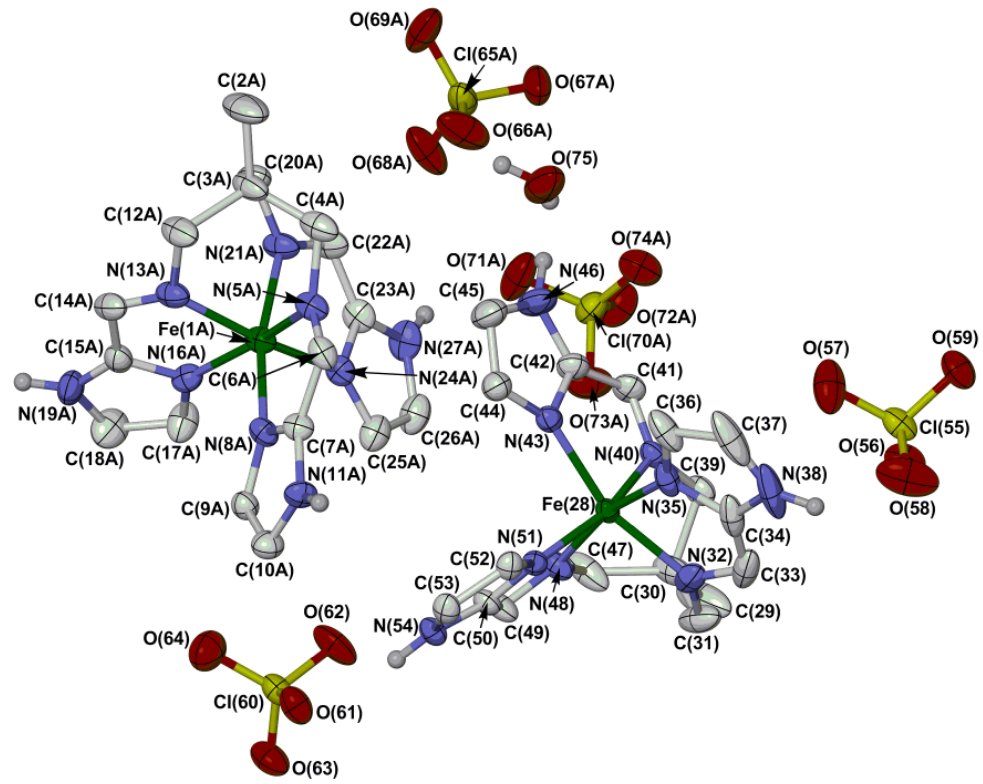


Fig. S1. Views of the asymmetric unit of $[Fe(IE)][ClO_4]_2 \cdot 0.7H_2O$, showing the 'A' (top) and 'B' (bottom) disorder orientations. Crystallographically ordered residues are the same in both views. All C-bound H atoms have been omitted for clarity, and displacement ellipsoids are at the 50% probability level. Colour code: C, white; H, grey; Cl, yellow; Fe, green; N, blue; O, red.

The crystallographically ordered water molecule is O(75), while the partial water site O(76B) is present in the 'B' disorder orientation only.

Table S1 Selected bond lengths and angles in the crystal structure of $[\text{Fe}(\text{IE})][\text{ClO}_4]_2 \cdot 0.7\text{H}_2\text{O}$ (\AA , $^\circ$). See Figure S1 for the atom numbering scheme. The two values given for parameters involving $\text{Fe}(1)$ correspond to the ‘A’ and ‘B’ disorder sites of this complex cation, respectively.

$\text{Fe}(1)-\text{N}(5)$	1.948(4), 1.937(6)	$\text{Fe}(28)-\text{N}(32)$	1.9614(16)
$\text{Fe}(1)-\text{N}(8)$	1.968(4), 2.006(6)	$\text{Fe}(28)-\text{N}(35)$	1.9785(15)
$\text{Fe}(1)-\text{N}(13)$	1.954(4), 1.968(5)	$\text{Fe}(28)-\text{N}(40)$	1.9641(14)
$\text{Fe}(1)-\text{N}(16)$	1.976(4), 1.964(6)	$\text{Fe}(28)-\text{N}(43)$	1.9856(15)
$\text{Fe}(1)-\text{N}(21)$	1.952(4), 1.945(7)	$\text{Fe}(28)-\text{N}(48)$	1.9481(16)
$\text{Fe}(1)-\text{N}(24)$	2.013(3), 2.004(4)	$\text{Fe}(28)-\text{N}(51)$	1.9956(13)
$\text{N}(5)-\text{Fe}(1)-\text{N}(8)$	80.16(17), 82.4(2)	$\text{N}(32)-\text{Fe}(28)-\text{N}(35)$	80.94(8)
$\text{N}(5)-\text{Fe}(1)-\text{N}(13)$	86.95(18), 88.5(2)	$\text{N}(32)-\text{Fe}(28)-\text{N}(40)$	85.47(6)
$\text{N}(5)-\text{Fe}(1)-\text{N}(16)$	164.62(16), 167.2(2)	$\text{N}(32)-\text{Fe}(28)-\text{N}(43)$	161.72(6)
$\text{N}(5)-\text{Fe}(1)-\text{N}(21)$	89.26(18), 85.2(2)	$\text{N}(32)-\text{Fe}(28)-\text{N}(48)$	88.38(8)
$\text{N}(5)-\text{Fe}(1)-\text{N}(24)$	104.82(14), 101.83(17)	$\text{N}(32)-\text{Fe}(28)-\text{N}(51)$	105.80(6)
$\text{N}(8)-\text{Fe}(1)-\text{N}(13)$	100.81(15), 108.2(2)	$\text{N}(35)-\text{Fe}(28)-\text{N}(40)$	101.14(6)
$\text{N}(8)-\text{Fe}(1)-\text{N}(16)$	93.11(17), 94.3(2)	$\text{N}(35)-\text{Fe}(28)-\text{N}(43)$	89.64(7)
$\text{N}(8)-\text{Fe}(1)-\text{N}(21)$	166.25(19), 160.7(2)	$\text{N}(35)-\text{Fe}(28)-\text{N}(48)$	165.91(7)
$\text{N}(8)-\text{Fe}(1)-\text{N}(24)$	93.85(16), 87.4(2)	$\text{N}(35)-\text{Fe}(28)-\text{N}(51)$	93.25(6)
$\text{N}(13)-\text{Fe}(1)-\text{N}(16)$	80.71(19), 80.7(3)	$\text{N}(40)-\text{Fe}(28)-\text{N}(43)$	80.99(6)
$\text{N}(13)-\text{Fe}(1)-\text{N}(21)$	87.25(19), 86.2(3)	$\text{N}(40)-\text{Fe}(28)-\text{N}(48)$	87.05(6)
$\text{N}(13)-\text{Fe}(1)-\text{N}(24)$	162.64(17), 162.4(2)	$\text{N}(40)-\text{Fe}(28)-\text{N}(51)$	163.05(6)
$\text{N}(16)-\text{Fe}(1)-\text{N}(21)$	99.21(19), 100.8(2)	$\text{N}(43)-\text{Fe}(28)-\text{N}(48)$	103.06(7)
$\text{N}(16)-\text{Fe}(1)-\text{N}(24)$	89.32(15), 90.4(2)	$\text{N}(43)-\text{Fe}(28)-\text{N}(51)$	90.26(6)
$\text{N}(21)-\text{Fe}(1)-\text{N}(24)$	80.31(19), 80.6(3)	$\text{N}(48)-\text{Fe}(28)-\text{N}(51)$	80.77(6)

Table S2 Selected bond lengths and angles in the crystal structure of $[\text{Fe}(\text{IF})][\text{BF}_4]_2$ (\AA , $^\circ$). The atom numbering scheme for this structure is shown in Fig. 1 of the main paper.

$\text{Fe}(1)-\text{N}(5)$	1.9831(18)	$\text{Fe}(1)-\text{N}(17)$	1.9995(19)
$\text{Fe}(1)-\text{N}(8)$	2.0206(18)	$\text{Fe}(1)-\text{N}(23)$	1.9714(18)
$\text{Fe}(1)-\text{N}(14)$	1.9849(18)	$\text{Fe}(1)-\text{N}(26)$	1.9993(19)
$\text{N}(5)-\text{Fe}(1)-\text{N}(8)$	80.75(7)	$\text{N}(8)-\text{Fe}(1)-\text{N}(26)$	90.52(7)
$\text{N}(5)-\text{Fe}(1)-\text{N}(14)$	86.69(7)	$\text{N}(14)-\text{Fe}(1)-\text{N}(17)$	80.78(8)
$\text{N}(5)-\text{Fe}(1)-\text{N}(17)$	163.62(7)	$\text{N}(14)-\text{Fe}(1)-\text{N}(23)$	85.99(8)
$\text{N}(5)-\text{Fe}(1)-\text{N}(23)$	86.60(7)	$\text{N}(14)-\text{Fe}(1)-\text{N}(26)$	161.52(7)
$\text{N}(5)-\text{Fe}(1)-\text{N}(26)$	105.42(7)	$\text{N}(17)-\text{Fe}(1)-\text{N}(23)$	102.89(7)
$\text{N}(8)-\text{Fe}(1)-\text{N}(14)$	105.40(8)	$\text{N}(17)-\text{Fe}(1)-\text{N}(26)$	89.40(8)
$\text{N}(8)-\text{Fe}(1)-\text{N}(17)$	92.40(8)	$\text{N}(23)-\text{Fe}(1)-\text{N}(26)$	80.97(8)
$\text{N}(8)-\text{Fe}(1)-\text{N}(23)$	162.34(7)		

Table S3 Selected bond lengths and angles in the crystal structure of $[\text{Fe}(\mathbf{IG})][\text{ClO}_4]_2$ (\AA , $^\circ$). The atom numbering scheme for this structure is shown in Fig. 2 of the main paper.

Fe(1)–N(5)	1.9578(9)	Fe(1)–N(16)	1.9831(9)
Fe(1)–N(8)	1.9941(9)	Fe(1)–N(21)	1.9618(9)
Fe(1)–N(13)	1.9540(10)	Fe(1)–N(24)	1.9834(10)
N(5)–Fe(1)–N(8)	79.69(4)	N(8)–Fe(1)–N(24)	93.49(4)
N(5)–Fe(1)–N(13)	87.98(4)	N(13)–Fe(1)–N(16)	79.76(4)
N(5)–Fe(1)–N(16)	164.41(4)	N(13)–Fe(1)–N(21)	85.96(4)
N(5)–Fe(1)–N(21)	87.36(4)	N(13)–Fe(1)–N(24)	162.15(4)
N(5)–Fe(1)–N(24)	102.03(4)	N(16)–Fe(1)–N(21)	101.21(4)
N(8)–Fe(1)–N(13)	102.91(4)	N(16)–Fe(1)–N(24)	92.36(4)
N(8)–Fe(1)–N(16)	93.61(4)	N(21)–Fe(1)–N(24)	79.85(4)
N(8)–Fe(1)–N(21)	163.93(4)		

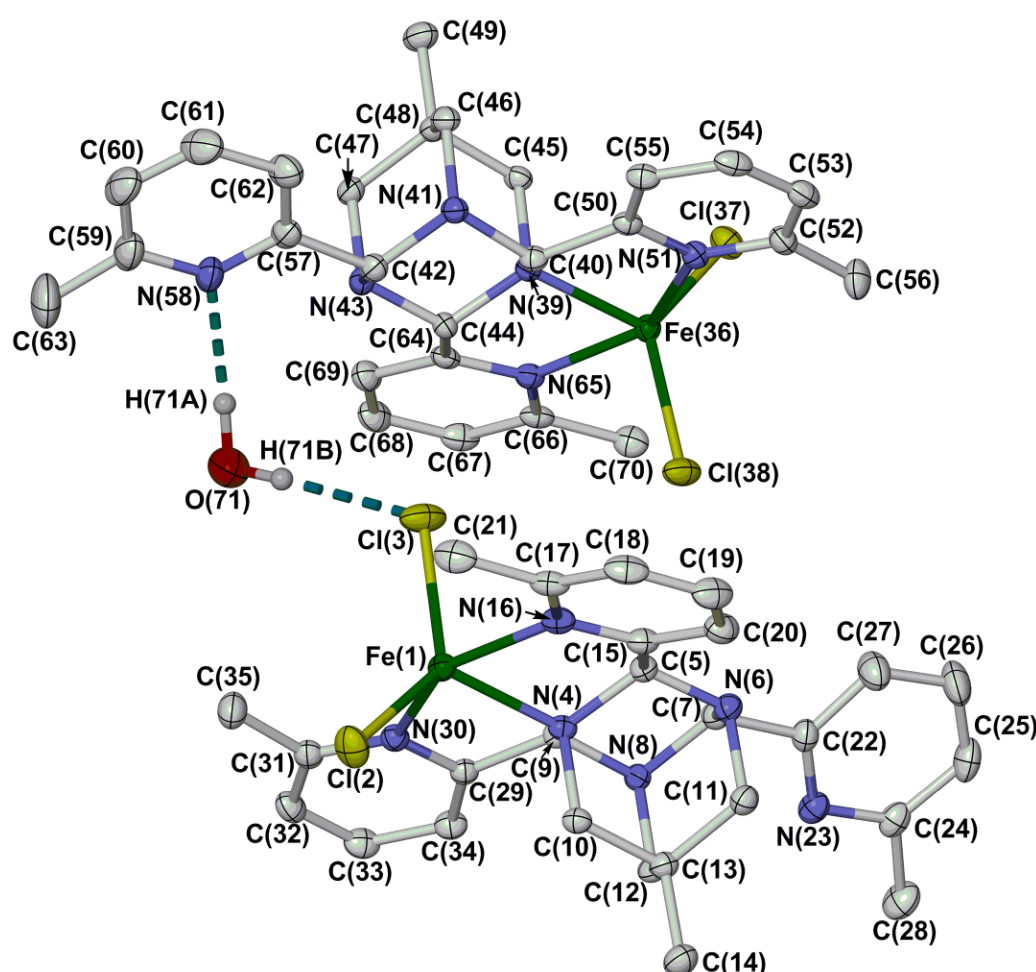


Fig. S2. View of the dimeric moiety in the crystal structure of $[\text{FeCl}_2(\mathbf{2C})]\cdot n\text{H}_2\text{O}$, showing the complete atom numbering scheme. Atomic displacement ellipsoids are at the 50 % probability level, and all C-bound H atoms have been omitted for clarity. Colour code: C, white; H, grey; Cl, yellow; Fe, green; N, blue; O, red.

Alternative views of this compound are presented in Figs. 5 and 6 of the main paper.

Table S4 Selected bond lengths and angles in the crystal structure of $[\text{FeCl}_2(\mathbf{2C})]\cdot n\text{H}_2\text{O}$ (\AA , $^\circ$). The full atom numbering scheme for this structure is shown in Fig. S2.

Fe(1)–Cl(2)	2.2915(7)	Fe(36)–Cl(37)	2.3231(6)
Fe(1)–Cl(3)	2.3796(7)	Fe(36)–Cl(38)	2.3625(6)
Fe(1)–N(4)	2.1380(18)	Fe(36)–N(39)	2.1365(17)
Fe(1)–N(16)	2.3413(18)	Fe(36)–N(51)	2.3004(17)
Fe(1)–N(30)	2.3137(17)	Fe(36)–N(65)	2.3364(17)
Cl(2)–Fe(1)–Cl(3)	128.86(3)	Cl(37)–Fe(36)–Cl(38)	129.35(3)
Cl(2)–Fe(1)–N(4)	120.02(5)	Cl(37)–Fe(36)–N(39)	116.76(5)
Cl(2)–Fe(1)–N(16)	100.77(5)	Cl(37)–Fe(36)–N(51)	98.00(5)
Cl(2)–Fe(1)–N(30)	97.27(5)	Cl(37)–Fe(36)–N(65)	98.76(5)
Cl(3)–Fe(1)–N(4)	111.12(5)	Cl(38)–Fe(36)–N(39)	113.86(5)
Cl(3)–Fe(1)–N(16)	91.65(5)	Cl(38)–Fe(36)–N(51)	92.91(5)
Cl(3)–Fe(1)–N(30)	95.04(5)	Cl(38)–Fe(36)–N(65)	96.00(4)
N(4)–Fe(1)–N(16)	74.75(6)	N(39)–Fe(36)–N(51)	75.33(6)
N(4)–Fe(1)–N(30)	75.99(6)	N(39)–Fe(36)–N(65)	74.27(6)
N(16)–Fe(1)–N(30)	150.45(6)	N(51)–Fe(36)–N(65)	149.38(6)
τ^a	0.360(1)	τ^b	0.334(1)

^a $\tau = \{[\text{N}(16)–\text{Fe}(1)–\text{N}(30)] – [\text{Cl}(2)–\text{Fe}(1)–\text{Cl}(3)]\} / 60^\circ$

^b $\tau = \{[\text{N}(51)–\text{Fe}(36)–\text{N}(65)] – [\text{Cl}(37)–\text{Fe}(36)–\text{Cl}(38)]\} / 60^\circ$

1. A. W. Addison, T. N. Rao, J. Reedijk, J. van Rijn and G. C. Verschoor, *J. Chem. Soc., Dalton Trans.*, 1984, 1349. An ideal square pyramidal structure gives $\tau = 0$, while a perfect trigonal pyramidal geometry gives $\tau = 1$.

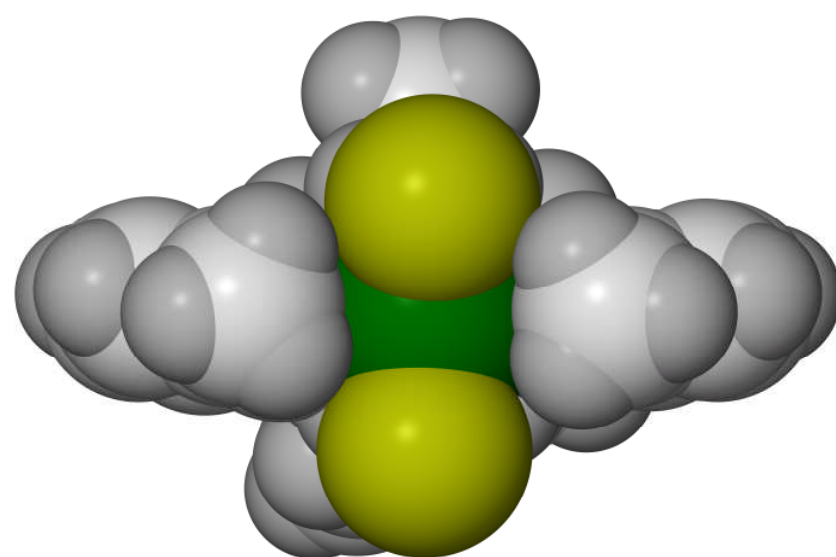


Fig. S3 Space-filling view of molecule 1 in $[\text{FeCl}_2(\mathbf{2C})]\cdot n\text{H}_2\text{O}$, showing the steric influence of the ligand methyl substituents on the iron coordination geometry. Colour code: C, white; H, grey; Cl, yellow; Fe, green; N, blue.

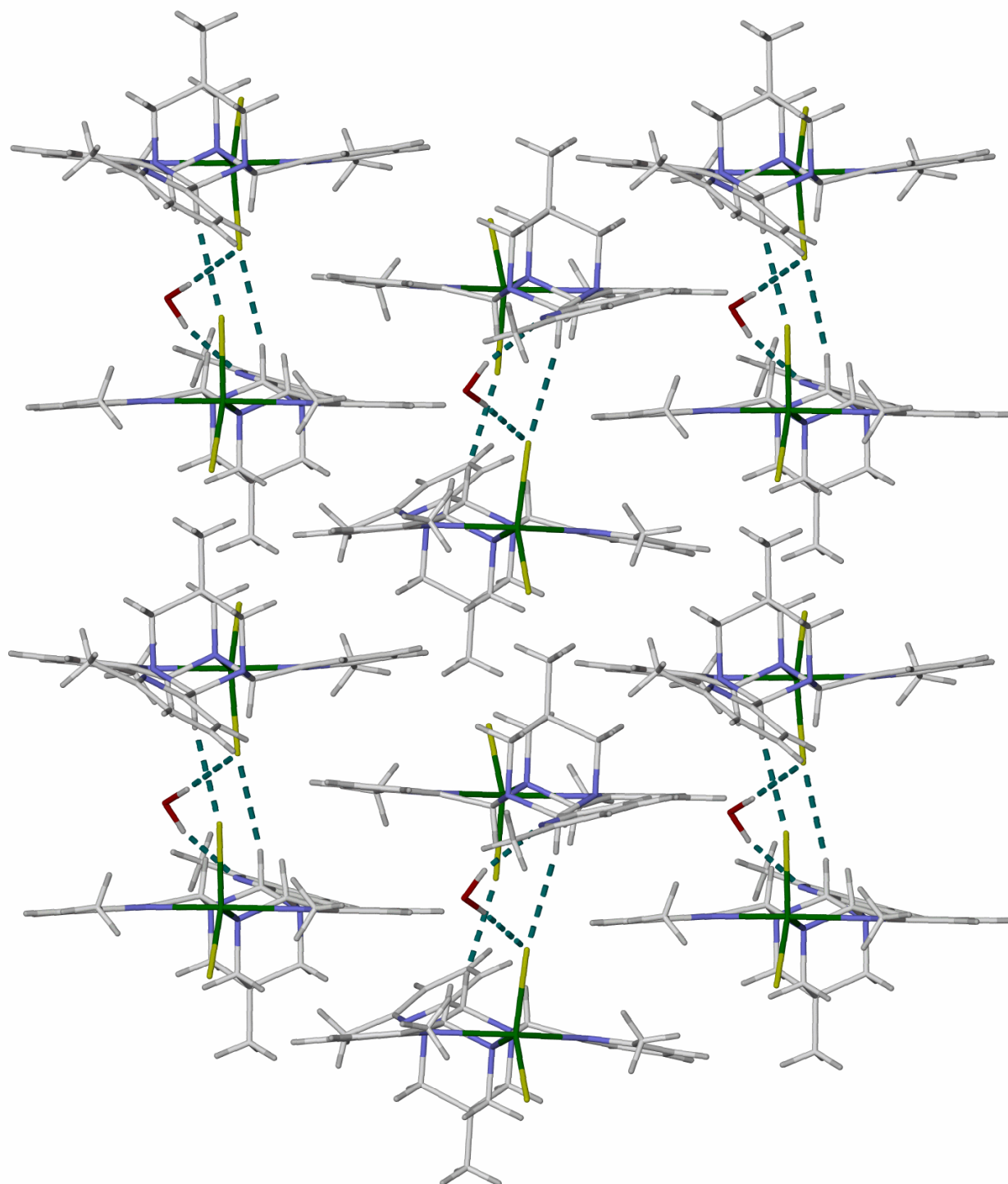


Fig. S4 Packing diagram of $[FeCl_2(2C)] \cdot nH_2O$, showing the interdigitation of the dimers into sheets of stacks through $\pi-\pi$ interactions. Colour code: C, white; H, grey; Cl, yellow; Fe, green; N, blue; O, red.

These sheets are in turn linked into three dimensions by another $\pi-\pi$ interaction, between the pendant pyridyl group C(57)-C(62) (Fig. S2) and its symmetry equivalent related by the crystallographic inversion centre.

Metric parameters for these $\pi-\pi$ interactions are given in Table S5.

Table S5 Metric parameters for the intermolecular π - π interactions in $[\text{FeCl}_2(\mathbf{2C})]\cdot n\text{H}_2\text{O}$ (\AA , $^\circ$).^a The full atom numbering scheme for this structure is shown in Fig. S2.

	Dihedral angle	Interplanar distance	Horizontal offset
$[\text{C}(15)\text{-C}(20)]\dots[\text{C}(29^{\text{ii}})\text{-C}(34^{\text{ii}})]$	3.59(6)	3.556(8)	2.05
$[\text{C}(15)\text{-C}(20)]\dots[\text{C}(64^{\text{iii}})\text{-C}(69^{\text{iii}})]$	12.80(5)	3.401(7)	1.59
$[\text{C}(50)\text{-C}(55)]\dots[\text{C}(64^{\text{iii}})\text{-C}(69^{\text{iii}})]$	4.08(6)	3.328(6)	0.88
$[\text{C}(50)\text{-C}(55)]\dots[\text{C}(29^{\text{ii}})\text{-C}(34^{\text{ii}})]$	5.63(6)	3.469(6)	1.36
$[\text{C}(57)\text{-C}(62)]\dots[\text{C}(57^{\text{iv}})\text{-C}(62^{\text{iv}})]$	0	3.360(2)	2.19

^aSymmetry codes: (ii) $\frac{1}{2}-x$, $\frac{1}{2}+y$, $\frac{1}{2}-z$. (iii) $\frac{3}{2}-x$, $\frac{1}{2}+y$, $\frac{1}{2}-z$. (iv) $1-x$, $2-y$, $-z$.

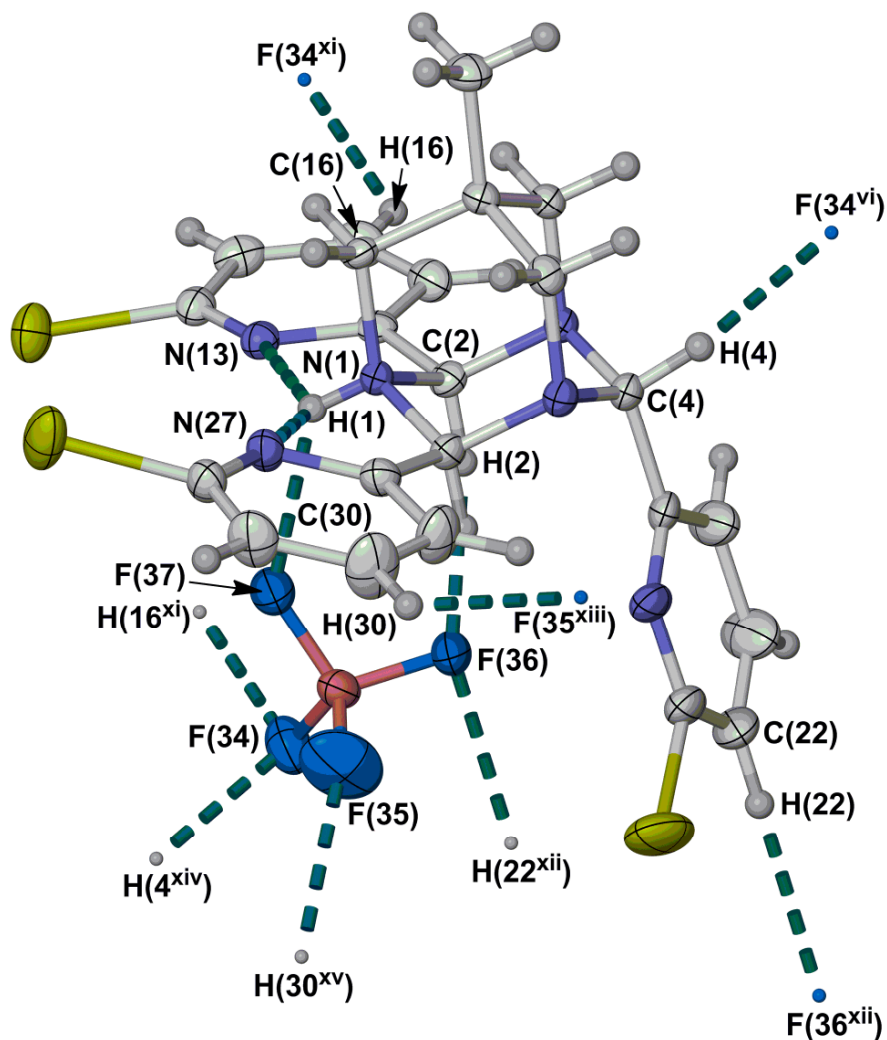


Fig. S5 View of the asymmetric unit in the crystal structure of $[2\text{BH}]\text{BF}_4$, showing the hydrogen-bonding interactions in the crystal lattice (Table S4). Displacement ellipsoids are at the 50% probability level apart from hydrogen atoms, which have arbitrary radii. Only atoms involved in hydrogen bonding interactions are labelled. Colour code: C, white; H, grey; B, pink; Br, yellow; F, cyan; N, blue.

Symmetry codes: (vi) $x, 1+y, z$; (xi) $1-x, 1-y, 1-z$; (xii) $-x, 1-y, 1-z$; (xiii) $-x, \frac{1}{2}+y, \frac{1}{2}-z$; (xiv) $x, -1+y, z$; (xv) $-x, -\frac{1}{2}+y, \frac{1}{2}-z$.

The hydrogen bonds form a $(4^6 6^5)_2$ network, in which the cations and the anions are both five-connected

Table S6 Hydrogen bond parameters for the crystal structures in this work (Å, °).^a The atom numbering schemes for the structures are shown in Figs. S1, S5 and Figs. 2 and 6 of the main paper.

	D–H	H...A	D...A	D–H...A
[Fe(IE)][ClO ₄] ₂ ·0.7H ₂ O				
N(11A)–H(11A)...O(59) ^v	0.88	2.37	3.118(13)	143.2
N(19A)–H(19A)...O(67A) ^{vi}	0.88	2.25	3.058(8)	152.8
N(19A)–H(19A)...O(75) ^{vi}	0.88	2.42	3.079(6)	132.2
N(27A)–H(27A)...O(71A)	0.88	2.30	3.114(5)	154.7
N(11B)–H(11B)...O(59) ^v	0.88	2.22	3.07(2)	163.9
C(12B)–H(12B)...O(71) ^{vii}	0.99	2.13	2.960(6)	140.1
C(12B)–H(12B)...O(73) ^{vii}	0.99	2.15	2.960(6)	137.6
C(12B)–H(12B)...O(74) ^{vii}	0.99	2.25	3.119(8)	146.5
N(19B)–H(19B)...O(67B) ^{vi}	0.88	2.45	2.900(13)	112.6
N(19B)–H(19B)...O(75) ^{vi}	0.88	1.93	2.628(6)	134.7
N(27B)–H(27B)...O(76B)	0.88	1.91	2.783(7)	170.2
C(37)–H(37)...O(57)	0.95	2.44	3.306(3)	151.3
N(38)–H(38)...O(56)	0.88	2.43	3.096(2)	133.0
N(46)–H(46)...O(75)	0.88	2.02	2.871(3)	162.3
N(54)–H(54)...O(61)	0.88	2.08	2.940(2)	167.0
O(75)–H(75A)...O(68A)	0.853(18)	2.25(3)	2.848(5)	127(3)
O(75)–H(75A)...O(69A) ^{viii}	0.853(18)	2.18(3)	2.856(4)	136(3)
O(75)–H(75B)...O(71A)	0.893(18)	2.29(3)	3.102(5)	151(3)
O(75)–H(75B)...O(74A)	0.893(18)	2.27(3)	2.923(4)	130(3)
O(75)–H(75A)...O(68B)	0.853(18)	2.55(3)	3.041(5)	117(3)
O(75)–H(75B)...O(76B)	0.893(18)	2.59(3)	3.215(8)	127(3)
O(76B)...O(71B) ^b	—	—	3.016(7)	—
O(76B)...O(72B) ^b	—	—	3.090(8)	—
O(76B)...O(69B) ^{ix,b}	—	—	3.020(9)	—
O(76B)...O(76B) ^{x,b}	—	—	2.814(11)	—
[Fe(IG)][ClO ₄] ₂				
N(9)–H(9)...O(29)	0.88	2.16	2.9427(15)	148.1
N(17)–H(17)...O(37)	0.88	2.11	2.9332(15)	155.4
N(25)–H(25)...O(31) ⁱ	0.88	2.02	2.8779(16)	163.6
[FeCl ₂ (2C)] _n H ₂ O				
C(7)–H(7)...Cl(38)	1.00	2.77	3.749(2)	166.6
C(42)–H(42)...Cl(3)	1.00	2.90	3.880(2)	167.8
O(71)–H(71A)–N(58)	0.94(5)	2.44(5)	3.379(3)	175(4)
O(71)–H(71B)–Cl(3)	0.95(4)	2.09(4)	3.016(3)	165(3)
[2BH]BF ₄				
N(1)–H(1)–N(13)	0.83(3)	2.45(3)	2.732(3)	101(2)
N(1)–H(1)–N(27)	0.83(3)	2.50(3)	2.754(3)	99(2)
N(1)–H(1)–F(37)	0.83(3)	2.33(3)	2.902(3)	127(3)
C(2)–H(2)–F(36)	1.00	2.22	3.186(3)	163.1
C(4)–H(4)–F(34) ^{vi}	1.00	2.31	3.128(3)	138.4
C(16)–H(16)–F(34) ^{xi}	0.95	2.47	3.153(3)	128.4
C(22)–H(22)–F(36) ^{xii}	0.95	2.47	3.413(4)	173.4
C(30)–H(30)–F(35) ^{xiii}	0.95	2.38	3.164(4)	140.2

^aSymmetry codes: (i) $-x, -y, -z$; (v) $1-x, -y, -z$; (vi) $x, 1+y, z$; (vii) $-1+x, 1+y, z$; (viii) $1-x, -y, 1-z$; (ix) $1+x, y, z$; (x) $2-x, -y, 1-z$; (xi) $1-x, 1-y, 1-z$; (xii) $-x, 1-y, 1-z$; (xiii) $-x, \frac{1}{2}+y, \frac{1}{2}-z$.

^bPotential hydrogen bond acceptors for the partial water molecule O(76B).

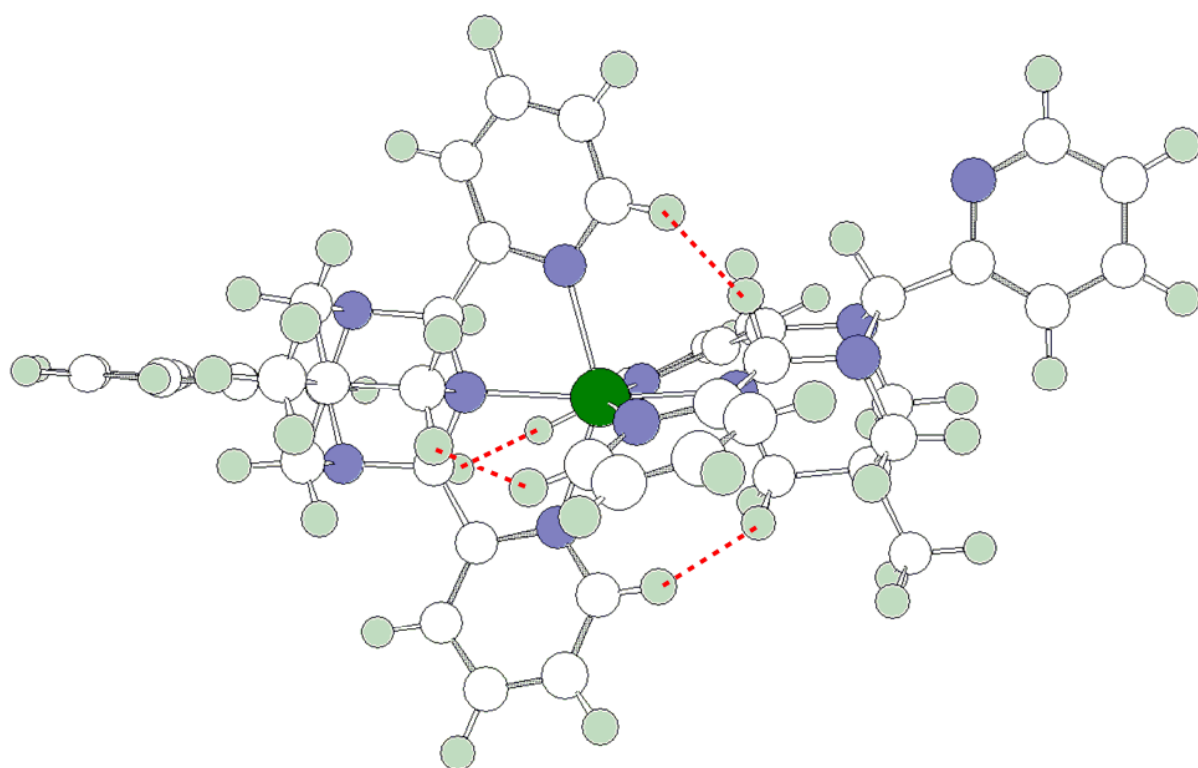


Fig. S6 Energy-minimised (MM2) molecular model of $[Fe(2A)_2]^{2+}$, highlighting the unfavourable steric contacts between the pyridyl groups of one ligand, and the adamantyl core of the other. The marked H...H distances are $<2.0\text{ \AA}$. The Fe–N bond lengths in the model are consistent with a high-spin iron centre; the steric clashes would be worse if the metal were low-spin.

These steric interactions are reduced, but not removed, by replacing the **2A** pyridyl groups with smaller, five-membered heterocyclic donors like imidazolyl groups.